Laser-based Cooperative Estimation of Pose and Size of Moving Objects using Multiple Mobile Robots

Yuto Tamura, Ryohei Murabayashi
Graduate School of Science and Engineering
Doshisha Unversity
Kyotanabe, Kyoto 610-0394 Japan

Masafumi Hashimoto, Kazuhiko Takahashi
Faculty of Science and Engineering
Doshisha Unversity
Kyotanabe, Kyoto 610-0394 Japan
e-mail: {mhashimo, katakaha}@mail.doshisha.ac.jp

***Abstract*—This paper presents laser-based tracking (estimation of pose and size) of moving objects using multiple mobile robots as sensor nodes. Each sensor node is equipped with a single-layer laser scanner and detects moving objects, such as people, cars, and bicycles, in its own laser-scanned images by applying an occupancy-grid-based method. Each sensor node then estimates the objects' poses (positions and velocities) and sizes using Bayesian filtering and sends these estimates to a central server. The central server combines the estimates to improve the tracking accuracy and then feeds the information back to the sensor nodes. In this cooperative-tracking method, the sensor nodes share their tracking information, allowing tracking of invisible or partially visible objects. The hierarchical architecture of cooperative tracking also makes the system scalable and robust. Experimental results using two sensor nodes confirm the performance of our tracking method.**

***Keywords*—moving-object tracking; cooperative tracking; pose and size estimation; laser scanner; mobile robot; sensor node**

I. INTRODUCTION

Tracking of multiple moving objects is an important issue in the safe navigation of mobile robots and vehicles. The use of laser scanners, radars, or stereo cameras in mobile robotics and vehicle automation has attracted considerable interest [1]–[7]. The term "tracking" means estimating the pose (position and velocity) and size of moving object throughout this paper.

Recently, numerous studies have been conducted on multirobot coordination and cooperation [8][9]. When multiple robots are located near each another, they can share their sensing data through communication network. The multirobot team can then be considered a multisensor system. Even if moving objects locate outside the sensing area of the robot are occluded, they can be found using tracking data from other robots in the team. Hence, multi robot system can improve the accuracy and reliability with which moving objects are tracked [10]–[16].

Such cooperative tracking or cooperative object localization can also be applied to vehicle automation, including intelligent transportation systems (ITS) and systems for personal mobility devices, as shown in Fig. 1. Cooperative tracking enables the detection of moving objects in the blind spot of each vehicle and can be used to detect sudden changes in a crowded urban environment such as people appearing on roads or vehicles making unsafe lane changes. It can therefore prevent traffic accidents.

Our previous works presented a cooperative people-tracking method in which multiple mobile robots or vehicles were used as mobile sensor nodes and equipped with laser scanners [17][18]. The covariance intersection method [19] was applied to operate the tracking system effectively in a decentralized manner without any central server. In cooperative people tracking, each person could be assumed to be a mass point because of the small size, and mass-point tracking (only the pose estimation) was then performed.

In the real world, several types of moving objects, such as people, cars, bicycles, and motorcycles, exist. Therefore, we should design a cooperative-tracking system for moving objects. In vehicle (car, motorcycle, and bicycle) tracking, we have to consider moving objects as rigid bodies and estimate both the poses and sizes to avoid the collisions in a crowded environment.

Figure 1. Example of cooperative tracking in urban environments.

 ISBN: 978-1-61208-518-0

Tracking of a rigid body is known as extended-object tracking, and many related studies have been conducted [20]–[24]. However, to the best of our knowledge, cooperative tracking using multiple mobile sensor nodes covers only mass-point tracking under the assumption that the tracked object is small. It estimates only the object's pose but does not estimate its size.

Therefore, we presented a laser-based cooperative-tracking method for rigid bodies that estimates both poses and sizes of people and vehicles using multiple mobile sensor nodes [25]. In a crowded environment, a vehicle is occluded or rendered partially visible by each sensor node. To correctly estimate the size of the vehicle, the laser measurements captured by sensor nodes in the team have to be merged. Our previous cooperative-tracking method for rigid bodies applied a centralized architecture. Each sensor node detected laser measurements related to the moving objects in its sensing area and transmitted the measurement information to a central server, which then estimated the poses and sizes of the objects. Such a centralized architecture imposes a computational burden upon the central server. Moreover, the architecture has a weakness for fault of communication system between sensor nodes and central server.

To address this problem, in this paper, we present a hierarchical method of cooperative tracking by which the poses and sizes of moving objects are locally estimated by the sensor nodes. Moreover, these estimates are then merged by a central server. The rest of the paper is organized as follows. Section II gives an overview of our experimental system. In Sections III and IV, cooperative tracking is discussed. In Section V, we describe an experiment in moving-object tracking using two mobile sensor nodes in an outdoor environment. We present our conclusions in Section VI.

II. Experimental System and Cooperative Tracking Overview

Fig. 2 shows the mobile-sensor node system used in our experiments. Each of the two sensor nodes has two independently driven wheels. A wheel encoder is attached to each drive wheel to measure its velocity. A yaw-rate gyro is attached to the chassis of each robot to sense the turning velocity. These internal sensors calculate the robot's pose using dead reckoning.

Each sensor node is equipped with a forward-looking laser scanner (SICK LMS100) to capture laser-scanned images that are represented by a sequence of distance samples in a horizontal plane of 270°. The angular resolution of the laser scanner is 0.5°, and each scan image comprises 541 distance samples. Each sensor node is also equipped with RTK–GPS (Novatel ProPak-V3 GPS). The sampling frequency of the sensors is 10 Hz.

We use broadcast communication over a wireless local area network to exchange information between the central server and the sensor nodes. The computer used in the sensor nodes and the central server is an Iiyama 15X7100-i7-VGB with a 2.8 GHz Intel core i7-4810MQ processor, and the operating system used is Microsoft Windows 7 Professional.

Figure 2. Overview of the mobile sensor node.

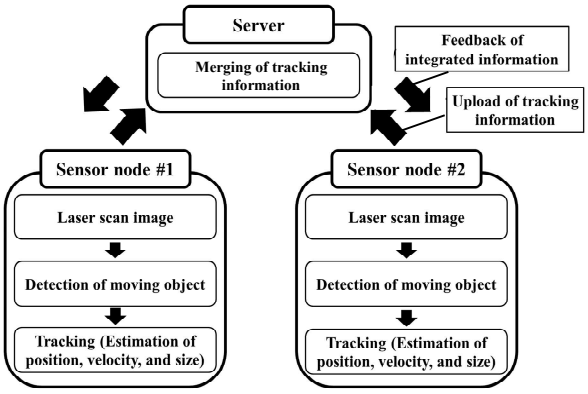

Figure 3. System overview of cooperative tracking.

Fig. 3 shows the sequence of moving-object tracking. Each sensor node independently finds the moving objects in its own laser-scanned images using an occupancy-grid method [26]. The sensor node then tracks the moving objects (estimates their poses and sizes), and the information is uploaded to the central server. The information includes the time stamp, the number of the objects tracked, and their pose and size. The central server merges the information. It estimates the poses and sizes of the moving objects using a Bayesian filter. The estimated information is then fed back to the sensor nodes.

To map the laser-scanned images onto the world coordinate frame (on which the grid map is represented), each sensor node accurately identifies its own position based on dead reckoning and GPS information using an extended Kalman filter [18].

III. Tracking by Sensor Node

In this section, we describe the process of estimating the poses and sizes of moving objects using Bayesian filter in conjunction with data association.

 ISBN: 978-1-61208-518-0

A. Pose and Size Estimation

We represent the shape of the moving object by a rectangle of width W and length L. We detail the size-estimation method in Fig. 4, where red circles indicate laser measurements of the moving object (hereafter, moving-object measurements), green lines are the feature lines extracted from those measurements, the green dashed rectangle is the estimated rectangle, and the green star is the centroid of that rectangle. As shown in Fig. 4, an $x_v y_v$-coordinate frame is defined, on which the y_v-axis aligns with the heading (orange arrow) of the tracked object. From the clustered moving-object measurements, we extract the width W_{meas} and length L_{meas}.

When a moving object is perfectly visible, its size can be estimated from these measurements. In contrast, when the object is partially occluded by other objects, its size cannot be accurately estimated. Therefore, the size of the partially occluded object is estimated by the following equation [20]:

$$\begin{cases} W_k = W_{k-1} + G(W_{meas} - W_{k-1}) \\ L_k = L_{k-1} + G(L_{meas} - L_{k-1}) \end{cases} \quad (1)$$

where W and L are estimates of width and length, respectively, and k and $k-1$ are time steps. G is the filter gain, given by $G = 1 - \sqrt[k]{(1-p)}$ [20], and p is a parameter. As the value of p increases, the reliabilities of the current measurements of W_{meas} and L_{meas} increase. We assume that a vehicle passes at 60 km/h in front of the sensor node. After the vehicle enters the surveillance area of the sensor node, we aim to estimate 99% of the size (p = 0.99) within 10 scans (1 s) of the laser scanner. We can then determine G as follows:

$$G = \begin{cases} 1 - \sqrt[k]{(1-0.99)} & \text{for } k \le 10 \\ 1 - \sqrt[10]{(1-0.99)} = 0.369 & \text{for } k > 10 \end{cases} \quad (2)$$

For a perfectly visible object, we set G = 1 in (1) and estimate its size.

The estimated size of the tracked object is used to classify the object as a person or a vehicle. If the estimated size in length or width is larger than 0.8 m, the object is assumed to be a vehicle. However, if the size is smaller than 0.8 m, it is assumed to be a person.

We then define the centroid position (green star in Fig. 4) of the rectangle estimated by (1). From the centroid position, the pose of the tracked object, position and velocity $(x, y, \dot{x}, \dot{y})$ on the world coordinate frame, is estimated using the Kalman filter under the assumption that the object is moving at an almost constant velocity.

To extract W_{meas} and L_{meas} from the moving-object measurements, we have to obtain the heading of the tracked object. As shown in Fig. 4, we extract two feature lines (green lines in Fig. 4) from the moving-object measurements using the split-and-merge method [27] and RANSAC [28] and determine the heading of the object from the orientations of the feature lines. When the two feature lines cannot be extracted, we determine the heading from the estimated velocity $(\dot{x}, \dot{y})$ of the object.

B. Data Association

To track objects in multi-object and multi-measurement environments, we apply data association (i.e., one-to-one matching of tracked objects and moving-object measurements). As shown in Fig. 5, a validation gate (validation region) is set around the predicted position (black circle) of each tracked object. The validation gate is rectangular, with a length and width 0.5 m greater than those of the object estimated at the previous time step (green dashed rectangle).

We refer to a representative point of grouped moving-object measurements (red and blue circles) as the representative measurement (light blue triangles). Representative measurements inside the validation gate are assumed to originate from the tracked object and are used to update the pose of the tracked object with the Kalman filter. Measurements outside the validation gate are identified as false and discarded.

Figs. 6 and 7, respectively, show an exemplary laser image and data association for a case in which two people move close to a car. In these figures, red circles indicate moving-object measurements, light blue triangles indicate representative measurements, black circles indicate tracked

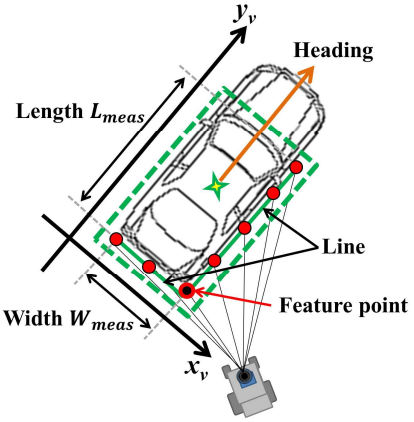

Figure 4. Size estimation of a vehicle.

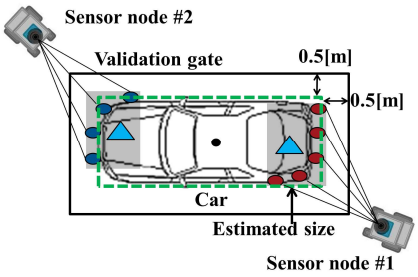

Figure 5. Laser images and data association.

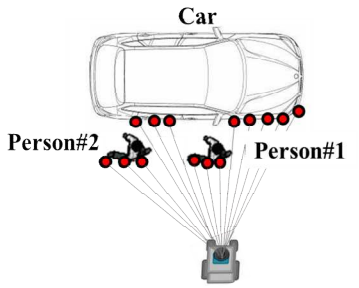

Figure 6. Laser images of a case in which two people are moving close to a car.

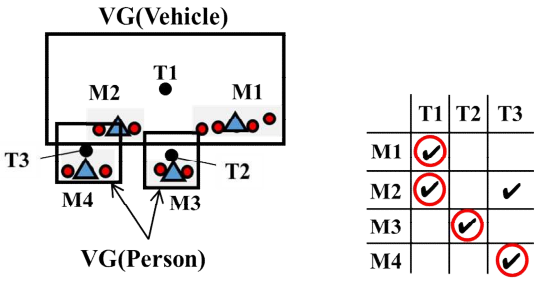

Figure 7. Data association for the laser images in Fig. 6.

objects, and VG stands for validation gate. The right table in Fig. 7 shows the correspondence between tracked objects and representative measurements.

As shown in Fig. 7, multiple representative measurements are often obtained inside a validation gate in the real world, and multiple tracked objects also compete for representative measurements. To achieve a reliable data association, we introduce the following rules:

a) Person: Because a person is small, he/she usually result in one representative measurement. Thus, if a tracked object is assumed to be a person, one-to-one matching of the tracked person and a representative measurement is performed.

b) Vehicle (car, motorcycle, or bicycle): Because a vehicle is large, as shown in Fig. 7, it often produces multiple representative measurements. Thus, if a tracked object is assumed to be a vehicle, one-to-many matching of the tracked vehicle and representative measurements is performed.

As shown in Fig. 6, on urban streets, people often move close to vehicles, whereas vehicles move far away from each other. Thus, when representative measurements of people exist in the validation gate of a tracked vehicle, they might be matched to the tracked vehicle. To avoid this, we begin data association for people.

We illustrate our data-association method from Fig. 7, in which the validation gates of a person and a car overlap. If tracked objects T2 and T3 are determined to be people, the representative measurement M3 is matched with T2 and the representative measurement M4 nearest to T3 is matched with T3, both through one-to-one matching. Subsequently, if the tracked object T1 is determined to be a vehicle, the two representative measurements M1 and M2 in the validation gate are matched with T1 through one-to-many matching. If the validation gates of several people overlap, one-to-one matching is performed using the global nearest neighbor method [18][29].

A representative measurement that is not matched with any tracked objects is assumed either to originate from a new moving object or to be a false alarm. Therefore, we tentatively initiate tracking of the measurement with the Kalman filter. If the measurement remains visible, it is assumed to originate from a new object and tracking is continued. If the measurement disappears quickly, it is treated as a false alarm, and tentative tracking is terminated.

Moving objects appear in and disappear from the sensing area of the laser scanner. They also occlude each other and are occluded by other objects in the environment. To maintain reliable tracking under such conditions, we implement a rule-based tracking-handling system [18].

IV. Merging of Tracking Data by a Central Server

The information concerning objects tracked by the sensor nodes is combined using data association. We present an example of our data-association procedure in Figs. 8 and 9, in which two sensor nodes are tracking a car. In Fig. 8, red and blue rectangles indicate the sizes of the tracked objects #A (TA) and #B (TB), as estimated by sensor nodes #1 and #2, respectively. Orange arrows indicate the headings of the objects.

If TA and TB originate from the same object, their position, velocity, and heading estimates will have similar values. If the tracked object is a vehicle, the size estimated by sensor nodes will be large. If it is a person, the estimated size will be small. Therefore, we set a validation gate with a constant radius of 3 m around the TA position (red star in Fig. 8) and introduce the following rules to match TB with TA:

a) Same or different object: When the estimated position of TB (blue star) is located within the validation gate, and the

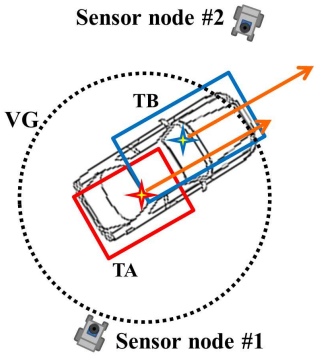

Figure 8. Data association of tracking information related to objects TA and TB.

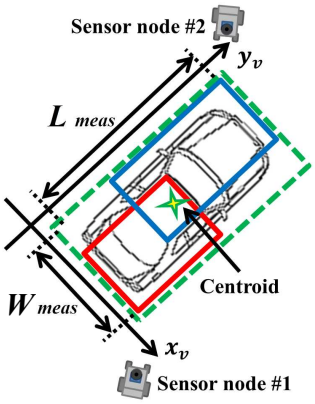

Figure 9. Integration of tracking information.

differences in the velocity and heading estimates of TA and TB are less than 0.8 m/s and 15°, respectively, the objects TA and TB are determined to originate from the same object. Otherwise, the objects TA and TB are determined to be different objects.

b) Vehicle or person: When the width and/or length estimates of the matched objects TA and TB are larger than 0.8 m, their objects are determined to originate from the same vehicle. When their width and length estimates are less than 0.8 m, the objects TA and TB are determined to originate from the same person.

When more than two tracked objects (e.g., TB and TC) are present in the validation gate of TA, the similar data association rules are applied.

After the two tracked objects TA and TB have been matched, their tracking information is combined. As shown in Fig. 9, we select the tracked object TB, which has a larger rectangle (blue rectangle) than TA (red rectangle), and define an $x_v y_v$-coordinate frame on which the y_v-axis aligns with the heading of TB. A rectangle (the green dashed rectangle) is then generated that encloses the two rectangles of TA and TB using positional information on their vertices. We then estimate the size of the integrated object using (1) based on the width and length of the new rectangle.

From the centroid position (green star) of the new rectangle, the position and velocity of the integrated object are estimated using the Kalman filter under the assumption that the object is moving at an almost constant velocity.

V. Experimental Results

We evaluated our cooperative-tracking method by conducting an experiment in a parking environment, as shown in Fig. 10. Two mobile sensor nodes tracked a car (vehicle #1), a motorcycle (vehicle #2), and two pedestrians (persons #1 and #2). Fig. 11 shows the movement paths of the sensor nodes (black dashed lines), vehicles #1 and #2 (blue and green lines), and persons #1 and #2 (red and black lines). The moving speeds of the sensor nodes, car, motorcycle, and people were approximately 1.5, 15, 20, and 6 km/h, respectively.

Fig. 12 (a) shows the position and size results estimated by cooperative tracking. We plot estimated rectangles every 1 s (10 scans). For comparison, individual tracking by each sensor node was also conducted. The tracking results for sensor nodes #1 and #2 are shown in Figs. 12 (b) and (c), respectively.

The estimated size of car (vehicle #1) using cooperative and individual tracking is shown in Figs. 13 (a), (b), and (c). In these figures, red and blue lines indicate the estimated length and width, respectively. Two dashed lines indicate

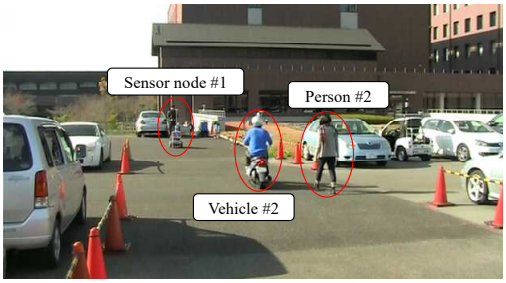

(a) Photo by camera #A

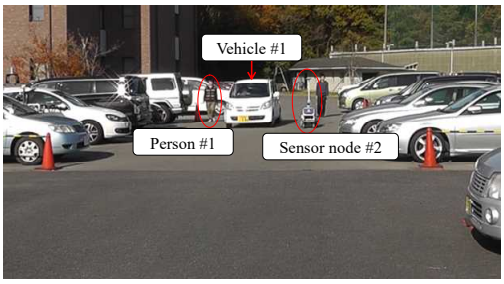

(b) Photo by camera #B

Figure 10. Photo of the experimental environment.

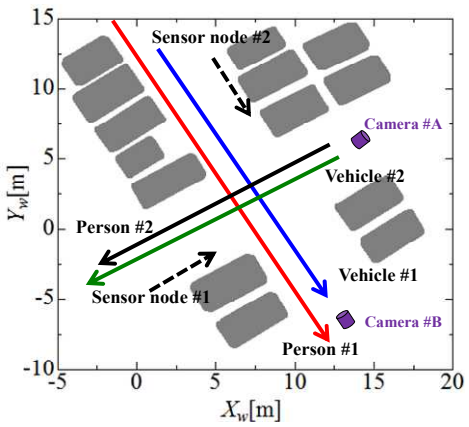

Figure 11. Movement paths of sensor nodes and moving objects

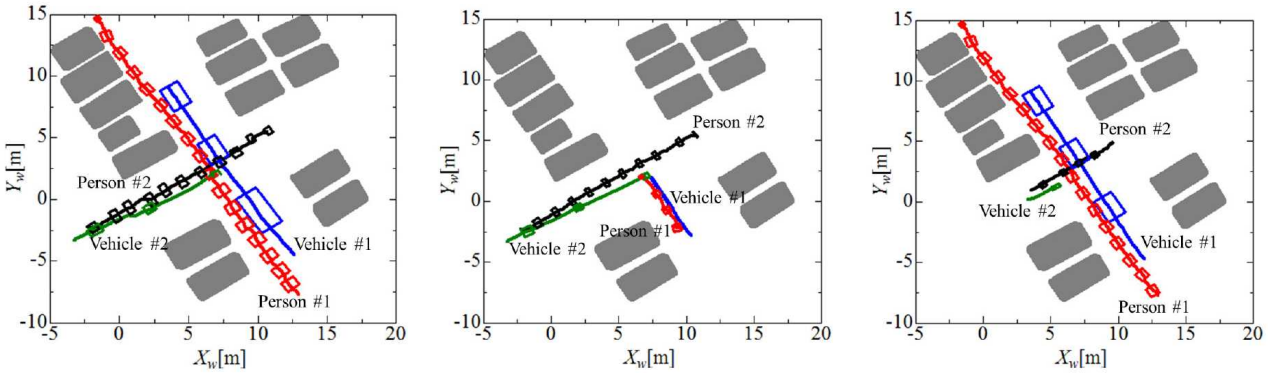

(a) Cooperative tracking (b) Individual tracking by sensor node #1 (c) Individual tracking by sensor node #2

Figure 12. Tracks and sizes of moving objects estimated by cooperative- and individual-tracking methods.

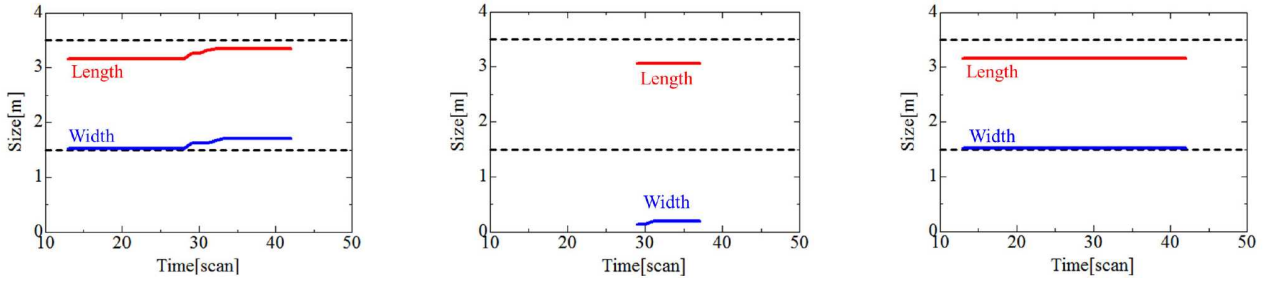

(a) Cooperative tracking (b) Individual tracking by sensor node #1 (c) Individual tracking by sensor node #2

Figure 13. Size of car (vehicle #1) estimated by cooperative- and individual-tracking methods.

TABLE I. PROCESSING TIME OF PROPOSED HIERARCHICAL COOPERATIVE TRACKING

	Maximum [ms]	Minimum [ms]	Mean [ms]
Central server	2.3	0.1	0.8
Sensor node #1	47.9	36.8	41.7
Sensor node #2	49.8	39.3	43.0

TABLE II. PROCESSING TIME OF PREVIOUS CENTRALIZED COOPERATIVE TRACKING

	Maximum [ms]	Minimum [ms]	Mean [ms]
Central server	23.8	2.2	7.9
Sensor node #1	41.5	36.1	38.2
Sensor node #2	45.7	36.5	38.8

the true length and width of the car.

In individual tracking, each sensor node partially tracks moving objects because the objects leave from the sensing area of the sensor nodes and are blocked by parked cars. In contrast, cooperative tracking always tracks the moving objects, because the two sensor nodes share the tracking data. It is clear from Figs. 12 and 13 that cooperative tracking offers better tracking accuracy than individual tracking.

We examined the processing times of the sensor nodes and the central server in the experiment. Tables I and II show the results of our proposed hierarchical tracking scheme and the previous centralized cooperative-tracking scheme, respectively.

In our previous method [25], the central server estimated the poses and sizes of moving objects based on the moving-objects measurements sent from the sensor nodes. Conversely, in our proposed method, the sensor nodes locally estimate the poses and sizes of moving objects, and the central server merges these estimates. Therefore, the hierarchical cooperative-tracking scheme reduces the computational burden on the central server.

VI. CONCLUSIONS

This paper presented a laser-based cooperative-tracking for moving objects using multiple mobile robots as sensor nodes. The moving objects were assumed to be rectangular rigid bodies, and the poses (positions and velocities) and sizes were locally estimated by the sensor nodes. These estimates were then merged by a central server. The effectiveness of such a hierarchical cooperative-tracking

method was demonstrated by an experiment in which a car, a motorcycle, and two pedestrians were tracked using two sensor nodes.

In this study, single-layer laser scanners on mobile sensor modes were used to sense the surrounding environments. Multilayer laser scanners provide richer information than single-layer laser scanners and thus improve recognition of the surrounding environment. Research is currently being conducted on the design of cooperative-tracking system using multiple sensor nodes equipped with multilayer laser scanners.

ACKNOWLEDGMENT

This study was partially supported by the Scientific Grants #26420213, the Japan Society for the Promotion of Science (JSPS), and the MEXT-Supported Program for the Strategic Research Foundation at Private Universities, 2014–2018, Ministry of Education, Culture, Sports, Science and Technology, Japan.

REFERENCES

[1] K. O. Arra and O. M. Mozos, Special issue on: People Detection and Tracking, Int. J. of Social Robotics, vol.2, no.1, 2010.

[2] C. Mertz, et al., "Moving Object Detection with Laser Scanners," J. of Field Robotics, vol.30, pp. 17–43, 2013.

[3] T. Ogawa, H. Sakai, Y. Suzuki, K. Takagi, and K. Morikawa, "Pedestrian Detection and Tracking using In-vehicle Lidar for Automotive Application," Proc. of IEEE Intelligent Vehicles Symp. (IV2011), pp. 734–739, 2011.

[4] A. Mukhtar, L. Xia, and T.B. Tang, "Vehicle Detection Techniques for Collision Avoidance Systems: A Review," IEEE Trans. on Intelligent Transportation Systems, vol. 16, pp. 2318–2338, 2015.

[5] H. Cho, Y. W. Seo, B.V.K. V. Kumar, and R. R. Rajkumar, "A Multi-sensor Fusion System for Moving Object Detection and Tracking in Urban Driving Environments," Proc. of Int. Conf. on IEEE Robotics and Automation (ICRA2014), pp. 1836–1843, 2014.

[6] D. Z. Wang, I. Posner, and P. Newman, "Model-free Detection and Tracking of Dynamic Objects with 2D Lidar," Int. J. of Robotics Research, vol.34, pp. 1039–1063, 2015

[7] D. Z. Wang, I. Posner, P. Newman, "What could move? Finding cars, pedestrians and bicyclists in 3D laser data," Proc. of IEEE Int. Conf. on Robotics and Automation (ICRA2012), pp. 4038–4044, 2012.

[8] Z. Yan, N. Jouandeau, and A. A. Cherif, "A Survey and Analysis of Multi-Robot Coordination," Int. J. of Advanced Robotic Systems, vol. 10, pp. 1–18, 2013.

[9] S. Nadarajah and K. Sundaraj, "A Survey on Team Strategies in Robot Soccer: Team Strategies and Role Description," Artificial Intelligence Review, vol. 40, pp. 271–304, 2013.

[10] Z.Wang and D. Gu, "Cooperative Target Tracking Control of Multiple Robots," IEEE Trans. on Industrial Electronics, vol. 59, pp. 3232–3240, 2012.

[11] K. Zhou and S. I. Roumeliotis, "Multirobot Active Target Tracking with Combinations of Relative Observations," IEEE Trans. on Robotics, vol. 27, pp. 678–695, 2011.

[12] A. Ahmad and P. Lima, "Multi-robot Cooperative Spherical-Object Tracking in 3D Space based on Particle Filters," Robotics and Autonomous Systems, vol. 61, pp. 1084–1093, 2013.

[13] P. U. Limaa, et al., "Formation Control Driven by Cooperative Object Tracking," Robotics and Autonomous Systems, vol. 63, Part 1, pp. 68–79, 2015.

[14] C. Robin and S. Lacroix, "Multi-robot Target Detection and Tracking: Taxonomy and Survey," Autonomous Robots, vol. 40, pp. 729–760, 2016.

[15] C. T. Chou, J. Y. Li, M. F. Chang, and L. C. Fu, "Multi-Robot Cooperation Based Human Tracking System Using Laser Range Finder," Proc. of IEEE Int. Conf. on Robotics and Automation (ICRA2011), pp. 532–537, 2011.

[16] N. A. Tsokas and K. J. Kyriakopoulos, "Multi-robot Multiple Hypothesis Tracking for Pedestrian Tracking," Autonomous Robot, vol. 32, pp. 63–79, 2012.

[17] K. Kakinuma, M. Hashimoto, and K. Takahashi, "Outdoor Pedestrian Tracking by Multiple Mobile Robots based on SLAM and GPS Fusion," Proc. of IEEE/SICE Int. Symp. on System Integration (SII2012), pp. 422–427, 2012.

[18] M. Ozaki, K. Kakinuma, M. Hashimoto, and K. Takahashi, "Laser-based Pedestrian Tracking in Outdoor Environments by Multiple Mobile Robots," Sensors, vol. 12, pp. 14489–14507, 2012.

[19] S.J. Julier and J.K. Uhlmann, "A Non-divergent Estimation Algorithm in the Presence of Unknown Correlations," Proc. of the IEEE American Control Conf., pp. 2369–2373, 1997.

[20] F. Fayad and V. Cherfaoui, "Tracking Objects using a Laser Scanner in Driving Situation based on Modeling Target Shape," Proc. of the 2007 IEEE Int. Vehicles Symp. (IV2007), pp. 44–49, 2007.

[21] T. Miyata, Y. Ohama, and Y. Ninomiya, "Ego-Motion Estimation and Moving Object Tracking using Multi-layer LIDAR," Proc. of IEEE Intelligent Vehicles Symp. (IV2009), pp. 151–156, 2009

[22] K. Granstrom, C. Lundquist, F. Gustafsson, and U. Orguner, "Radom Set Methods, Estimation of Multiple Extended Objects," IEEE Robotics & Automation Magazine, pp. 73–82, June 2014

[23] L. Mihaylova, et al., "Overview of Bayesian Sequential Monte Carlo Methods for Group and Extended Object Tracking," Digital Signal Processing, vol. 25, pp.1–16, 2014.

[24] J. Lan and X. R. Li, "Tracking of Extended Object or Target Group using Random Matrix Part I: New Model and Approach," Proc. of 15th Int. Conf. on Information Fusion (FUSION2012), pp.2177–2184, 2012.

[25] M. Hashimoto, R. Izumi, Y. Tamura, and K. Takahashi, "Laser-based Tracking of People and Vehicles by Multiple Mobile Robots," Proc. of the 11th Int. Conf. on Informatics in Control, Automation and Robotics (ICIT2014), pp. 522–527, 2014.

[26] M. Hashimoto, S. Ogata, F. Oba, and T. Murayama, "A Laser-based Multi-Target Tracking for Mobile Robot," Intelligent Autonomous Systems 9, pp. 135–144, 2006.

[27] V. Nguyen, A. Martinelli, N. Tomatis, and R. Siegwart, "A Comparison of Line Extraction Algorithms using 2D Laser Rangefinder for Indoor Mobile Robotics," Proc. of 2005 IEEE/RSJ Int. Conf. on Intelligent Robots and Systems (IROS2009), pp. 1929–1934, 2009.

[28] M. Fischler and R. Bolles, "Random Sample Consensus: A Paradigm for Model Fitting Applications to Image Analysis and Automated Cartography," Proc. of Image Understanding workshop, pp. 71–88, 1980.

[29] P. Konstantinova, A. Udvarev, and T. Semerdjiev, "A Study of a Target Tracking Algorithm Using Global Nearest Neighbor Approach," Proc. of Int. Conf. on Systems and Technologies, 2003.

 ISBN: 978-1-61208-518-0